

# Technical Notes

TECHNICAL NOTES are short manuscripts describing new developments or important results of a preliminary nature. These Notes cannot exceed 6 manuscript pages and 5 figures; a page of text may be substituted for a figure and vice versa. After informal review by the editors, they may be published within a few months of the date of receipt. Style requirements are the same as for regular contributions (see inside back cover).

## Numerical Study of Supersonic Turbulent Boundary Layer over a Small Protuberance

A. POLAK\*

University of Cincinnati, Cincinnati, Ohio

### Introduction

HIGH speed flow past external protuberances is characterized by interaction phenomena which alter the pressure distribution, cause locally high heating rates, and therefore are of considerable concern to the aerodynamicist. The presence of a protuberance will often be manifested by separation regions ahead and behind the protuberance and at high speed also by shock waves. This will certainly be the case for a large protuberance, which extends normal to the surface across the boundary layer into the high-speed external flow. On the other hand, a small protuberance is submerged in the boundary layer and separation may or may not occur, depending on the shape and size of the protuberance and local flow conditions. If the small protuberance is a design element attached to the surface of the vehicle, it can be faired so that it has a smooth junction with the skin and flow separation will not occur, especially when the boundary layer is turbulent. Even if the boundary layer remains attached the presence of the small protuberance will have a significant effect on the distribution of surface wall shear and heat transfer when the height of the protuberance is comparable to or larger than the boundary-layer displacement thickness. The nonmonotonic growth of the boundary layer also affects these distributions and the problem is therefore of an interactive nature.

From among the previous studies related to this problem area it is appropriate to mention here the experimental studies of Bertram et al.<sup>1,2</sup> Laminar and turbulent flows over small protuberances were investigated with emphasis on peak aerodynamic heating. Experimental data and also a semiempirical method to predict heating rates of attached turbulent flows over small protuberances are found in Ref. 3. In the present Note some of the results of a more exact numerical study of attached interacting supersonic turbulent boundary layers over a two-dimensional protuberance are presented. This is believed to be the first attempt to predict interacting turbulent flows by a finite-difference method.

### About the Solution Method

The supersonic turbulent boundary-layer flow over a single two-dimensional protuberance was considered. It was assumed that the developing boundary layer over the bump modifies significantly the pressure distribution so that the interaction

between the boundary layer and the external flow must be accounted for. The geometry of the protuberance was chosen to simulate flow over a flat plate with a two-dimensional bump. To avoid the argument about the validity of the boundary-layer equations at the junctions of the protuberance and the flat plate or the question about the downstream propagation of the disturbance induced at the junction points, we chose the normal distribution curve to represent the profile of the protuberance (see Fig. 1). Thus, the profile is described by  $y_w = h_1\{\phi(X) - \phi(-8)\}$  and where  $X = 8(x - 1.5)$  and the normal distribution function  $\phi$  is:  $\phi(X) = \exp(-X^2/2)/(2\pi)^{1/2}$ . The maximal value of the constant  $h_1$  used in our test cases was 0.10 with the corresponding  $y_{w,max} = h = 0.04$  at the crest of the protuberance ( $x = 1.5$ ). Notice that  $y_w = 0$  at  $x = 0.5$  and  $y_w(x = 1) = y_w(x = 2) = 1 \times 10^{-5}$  and the surface slope at  $x = 1$  is about  $0.02^\circ$ . Hence the width,  $w$ , of the protuberance was taken to be unity, extending from  $x = 1$  to  $x = 2$ . Therefore  $h/w = 0.04$  for  $h_1 = 0.10$ .

The governing turbulent boundary-layer equations were solved by the numerical implicit finite-difference method. In our approach we were drawing on previous studies of Refs. 4-6. We therefore delete the details of the mathematical formulation of the problem and the numerical techniques employed. Essentially, we combined the method of velocity averaging used by Wornom and Werle<sup>4</sup> to recover the weak interaction solution of the laminar boundary-layer equations with the method of Harris<sup>5</sup> to solve noninteracting laminar, transitional, and turbulent compressible boundary layers. The time-averaged turbulent boundary-layer equations for two-dimensional flow of a perfect gas were recast into the transformed nondimensional variables, using Levy-Lees independent variables.<sup>5-7</sup> A two-layer model was adopted to calculate the ratio of the eddy viscosity to the molecular viscosity. A streamwise intermittency distribution,  $\Gamma$ , was employed. With  $\Gamma = 0$  the governing equations reduced to represent exactly the laminar flow and with  $\Gamma = 1$  the fully turbulent flow was represented. In our calculations  $\Gamma = 0$  up to station  $x = 0.66$ . Constant Prandtl number = 0.72, and turbulent Prandtl number = 0.90 was taken, with the ratio of specific heats equal to 1.4. The equations were solved for a set of freestream Mach numbers,  $M_\infty$ , Reynolds numbers,  $Re_\infty$ , and ratio of wall-to-stagnation temperatures,  $T_w/T_{0,\infty}$ , and a constant freestream static temperature,  $T_\infty = 390^\circ R$ .

To represent properly the interaction between the viscous and inviscid flow, the pressure gradient was calculated as if the inviscid flow would pass over a displaced body, composed of the protuberance contour plus the boundary-layer displacement thickness.<sup>6</sup>

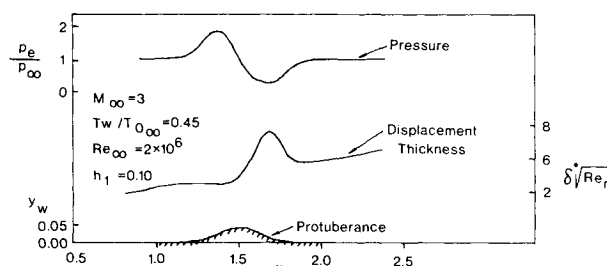


Fig. 1 Distribution of pressure and displacement thickness over a 2-D protuberance.

Received November 5, 1973; revision received March 6, 1974. This work was supported jointly by Naval Ordnance Laboratory, Applied Aerodynamics Division, Silver Spring, Md. and Naval Air Systems Command, AIR 320 under Contract N00019-73-C-0223. The author acknowledges with thanks M. J. Werle for the helpful discussions and S. D. Bertke for assistance in the computer effort.

Index categories: Boundary Layer and Convective Heat Transfer—Turbulent; Jets, Wakes, and Viscid-Inviscid Flow Interactions.

\* Associate Professor of Aerospace Engineering. Associate Fellow AIAA.

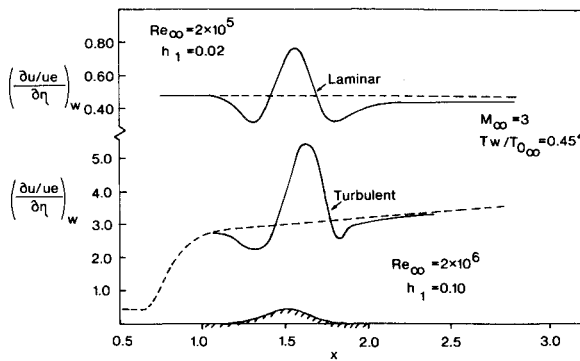


Fig. 2 Distribution of laminar and turbulent wall shear stress over a 2-D protuberance.

### Discussion of Results

Solutions to the governing turbulent boundary-layer equations were performed on the Naval Ordnance Laboratory CDC 6400 Computer with average computer time per test case of 10 min. Our interest was centered on the effect of Mach number, Reynolds number, and wall temperature on the distribution of surface heat-transfer coefficient  $q$  and skin-friction coefficient  $c_f$ . In Fig. 1 the sketch of the protuberance geometry, the distribution of the displacement thickness and pressure are presented for a test case with  $M_\infty = 3.0$ ,  $Re_\infty = \rho_\infty u_\infty / \mu_\infty = 2 \times 10^6$ ,  $T_w/T_\infty = 0.45$ , and  $h_1 = 0.10$ . The computation commences at  $x = 0.50$  assuming laminar weak-interacting flow. Transition starts at  $x = 0.66$  ( $\Gamma = 0$ ), with intermediate values of the intermittency  $\Gamma = 0.554$  at  $x = 0.80$ ,  $\Gamma = 0.991$  at  $x = 1.00$ ,  $\Gamma = 0.9997$  at  $x = 1.10$ . Therefore practically the boundary layer may be considered fully turbulent at  $x = 1.0$ . The nonmonotonic growth of the displacement thickness results in an asymmetrical pressure distribution around the crest of the protuberance and thus points to the need to account in such problems for the boundary-layer interaction displacement effect. The corresponding surface shear distribution is presented in the lower part of Fig. 2. The dashed curve in Fig. 2 represents the distribution of the wall shear parameter  $[\partial(u/u_e)/\partial\eta]_w$ , corresponding to the weak-interacting solution over a flat plate, under otherwise identical conditions. Observe the relatively fast recovery of the wall shear and its asymptotic approach to the flat plate, undisturbed values. A similar behavior was observed also in the experimental studies of turbulent heating over a single sine wave (Ref. 2, p. 1765). It is reported there that the heating quickly approached undisturbed flat plate heating values. For comparison a laminar shear distribution is shown at top of Fig. 2. Although the height of the protuberance is only one-fifth

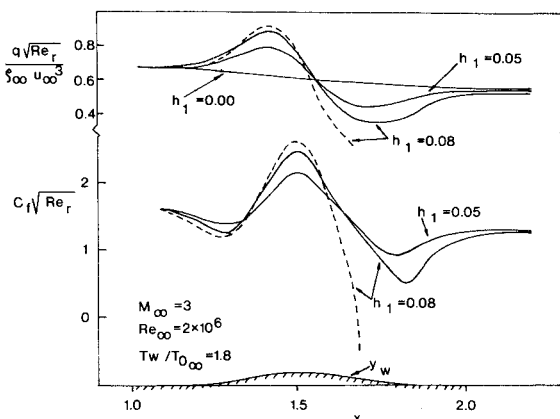


Fig. 3 Effect of  $h/\delta^*$  on turbulent heat transfer and skin friction.

Table 1 Comparison of peak heating rates

| $M_\infty$ | $Re_\infty \times 10^{-6}$ | $T_w/T_\infty$ | $h_1$ | $h/w$ | $h/\delta_{fp}^*$ | $\Delta q/q_{fp}$ |         |
|------------|----------------------------|----------------|-------|-------|-------------------|-------------------|---------|
|            |                            |                |       |       |                   | Present           | Eq. (1) |
| 2.0        | 2                          | 0.45           | 0.05  | 0.020 | 7.97              | 0.171             | 0.200   |
| 3.0        | 2                          | 0.45           | 0.05  | 0.020 | 4.83              | 0.286             | 0.274   |
| 4.0        | 2                          | 0.45           | 0.05  | 0.020 | 3.29              | 0.365             | 0.384   |
| 3.0        | 2                          | 0.45           | 0.10  | 0.040 | 9.65              | 0.545             | 0.545   |
| 3.0        | 2                          | 1.80           | 0.08  | 0.032 | 3.62              | 0.416             | 0.445   |
| 3.0        | 2                          | 1.80           | 0.05  | 0.020 | 2.27              | 0.260             | 0.268   |
| 3.0        | 2                          | 1.80           | 0.10  | 0.040 | 4.46              | 0.508             | 0.537   |
| 3.0        | 4                          | 0.45           | 0.10  | 0.040 | 12.23             | 0.529             | 0.552   |
| 3.0        | 10                         | 0.45           | 0.10  | 0.040 | 14.60             | 0.526             | 0.550   |

of that for a turbulent case, the downstream recovery zone for the laminar flow is considerably longer. The need to account for the effect of the displacement thickness is again demonstrated in Fig. 3. Here the distribution of skin friction  $c_f$  is obtained for the same conditions once as an interacting solution (full line) and secondly by neglecting the effect of the displacement thickness (dashed line). The noninteracting solution indicates separation erroneously. It was verified earlier<sup>4,6</sup> that for non-separating laminar boundary-layer problems governed by the boundary-layer equations with interaction valid solutions can be affected by the so-called "velocity-averaging" scheme. This method correctly accounts for the interaction process and at the same time suppresses the branching behavior toward a free interaction solution, used for separating boundary layers. This "interaction-with-averaging" algorithm proved to be applicable to the present turbulent boundary-layer problem.

A so-called shallow wave theory was developed by Savage and Nagel<sup>3</sup> to predict peak heating rates for attached laminar flow over a two-dimensional protuberance. It was later modified for turbulent flow through the use of some constants evaluated empirically. The following semiempirical formula was proposed:

$$\frac{q_{\max} - q_{fp}}{q_{fp}} = \frac{1}{2} \left\{ \frac{h}{wF} \left( 1 - \frac{\delta^*}{h} \right) - 2.5 + \left[ 6.25 + \frac{5h}{wF} \left( 1 + \frac{\delta^*}{h} \right) + \left( \frac{h}{wF} \right)^2 \left( 1 - \frac{\delta^*}{h} \right)^2 \right]^{1/2} \right\} \quad (1)$$

where  $q_{fp}$  = the corresponding undisturbed flat plate heating value at the same location as the peak value  $q_{\max}$  on the protuberance,  $\delta^*$  = flat plate turbulent boundary-layer displacement thickness at this location, and  $F \equiv (M_\infty^2 - 1)^{1/2} / \gamma \pi M_\infty^2$ . Equation (1) has been tested against the experimental data of Refs. 2 and 3. A comparison of this formula with the results obtained from our calculations are presented in Table 1. This comparison is quite favorable over the whole range of test conditions used in our calculations. We observe that for attached flow the increase in the peak heating rates above that for a flat plate is approximately proportional to the increase in  $h/\delta^*$ . The Mach number effect appears also to be strong. On the other hand, the direct effect of Reynolds number and wall temperature are not significant when the peak heating is compared to the corresponding local flat plate values. Future effort should be aimed at the study of separated laminar and turbulent boundary layers over two-dimensional protuberances.

### References

- Bertram, M. H. and Wiggs, M. M., "Effect of Surface Distortions on the Heat Transfer to a Wing at Hypersonic Speeds," *AIAA Journal*, Vol. 1, No. 6, June 1963, pp. 1313-1319.
- Bertram, M. H., Weinstein, L. M., Carry, A. M., Jr., and Arrington, J. P., "Heat Transfer to Wavy Wall in Hypersonic Flow," *AIAA Journal*, Vol. 5, No. 10, Oct. 1967, pp. 1760-1767.
- Jaek, C. L., "Analysis of Pressure and Heat Transfer Tests on Surface Roughness Elements with Laminar and Turbulent Boundary Layers," CR-537, Aug. 1966, NASA.
- Wornom, S. F. and Werle, M. J., "Displacement Interaction and

Surface Curvature Effects on Hypersonic Boundary Layers," *AIAA Journal*, Vol. 10, No. 12, Dec. 1972, pp. 1557-1558.

<sup>5</sup> Harris, J. E., "Numerical Solutions of the Equations for Compressible Laminar, Transitional and Turbulent Boundary Layers and Comparisons with Experimental Data," TR R-368, Aug. 1971, NASA.

<sup>6</sup> Werle, M. J., Polak, A., and Bertke, S. D., "Supersonic Boundary Layer Separations and Reattachment—Finite Difference Solutions," AFL 72-12-1, Jan. 1973, University of Cincinnati, Cincinnati, Ohio.

<sup>7</sup> Polak, A., "Interacting Supersonic Turbulent Boundary Layer over a Two-dimensional Protuberance," NOLTR 74-16, Jan. 1974, Naval Ordnance Laboratory, White Oak, Md.

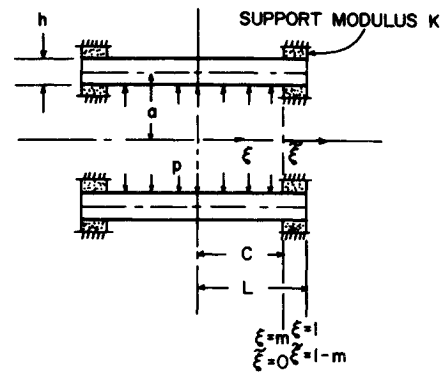


Fig. 1 Shell geometry and coordinate system.

## Flexure of Elastically Supported Axisymmetric Shells

S. T. GULATI\*

Corning Glass Works, Corning, N.Y.

AND

M. C. DOKMECI†

Deniz Harp Okulu, Istanbul, Turkey

### Introduction

THE present Note is concerned with the flexure of axisymmetric cylindrical shells with elastically supported edges. In particular, the effects of support parameters, namely support width and support stiffness, on the stress distribution throughout the shell are examined using Reissner-Naghdi shell theory.<sup>1,2</sup> In practice, one seldom encounters either rigidly clamped or simply supported edges. Indeed, in the case of shells made of brittle materials, it is undesirable and impractical to clamp the edges because of the presence of microcracks at the cut edges. On the other hand if the edges are simply supported, the maximum value of axial bending moment, for example, in a short uniformly loaded circular cylindrical shell is of substantial magnitude. Thus, by proper choice of the support parameters it should be possible to reduce the absolute value of maximum bending moment and to ascertain its location away from the edges. The analogous problem for rectangular plates has been treated by Gulati and Buehl,<sup>3</sup> while that for axisymmetric plates was examined by Reismann<sup>4</sup> and more recently by Gulati.<sup>5</sup>

Using the basic equations of Reissner-Naghdi shell theory, the general solution for the deflection and stress resultants is obtained for the region away from the support and the support region. The details of the solution are omitted; however, the results based on this solution are compared with those corresponding to axisymmetric cylindrical shells with simply supported or clamped edges. The effect of length/diam ratio and thickness/diam ratio on the stress resultants is examined for different values of support parameters. It is shown that many beneficial effects derive from elastic supports.

### Analysis

For the circular cylindrical shell, Fig. 1, of midsurface radius  $a$ , thickness  $h$ , and length  $2L$  supported elastically on gaskets of spring modulus  $K$  and width  $(L-c)$  and subjected to an internal pressure  $p$ , the basic equations of Reissner-Naghdi theory as modified by Essenburg<sup>6</sup> result in the following differential

equations for axial moment  $M_x$  in the inner and support regions respectively:

$$\phi^{iv} - 2(\omega^2 - \zeta^2)\eta^2\phi'' + 4\eta^4\phi = -(\nu/\lambda^2)(p/E)[1 - (\gamma/2\lambda)], \quad 0 \leq \xi \leq m \quad (1)$$

$$\tilde{\phi}^{iv} - 2(\tilde{\omega}^2 - \tilde{\zeta}^2)\tilde{\eta}^2\tilde{\phi}'' + 4\tilde{\eta}^4\tilde{\phi} = 0, \quad 0 \leq \tilde{\xi} \leq 1-m$$

where

$$\begin{aligned} \phi &= M_x/EL^2 = \bar{M}_x & m &= c/L \\ \tilde{\phi} &= \tilde{M}_x/EL^2 = \tilde{\bar{M}}_x & K' &= K(L-c) \\ \gamma &= h/L & \xi &= x/L \\ \lambda &= a/L & \tilde{\xi} &= \xi - m \\ \omega^2, \tilde{\omega}^2 &= 1 + \rho^2(\eta^2/\mu^2), & 1 + \tilde{\rho}^2(\tilde{\eta}^2/\mu^2) \\ \zeta^2, \tilde{\zeta}^2 &= 1 - \rho^2(\eta^2/\mu^2), & 1 - \tilde{\rho}^2(\tilde{\eta}^2/\mu^2) \\ \rho^2, \tilde{\rho}^2 &= 1 - \frac{\nu\gamma^2\mu^2}{12(1-\nu^2)}, & 1 - \frac{\nu\gamma^2\mu^2}{12(1-\nu^2)\Omega^4} \\ \eta^4, \tilde{\eta}^4 &= \frac{3(1-\nu^2)}{\gamma^2\lambda^2}, & \frac{3(1-\nu^2)\Omega^4}{\gamma^2\lambda^2} \\ \mu^2 &= \frac{5(1-\nu)}{\gamma^2}, & \Omega^4 &= 1 + \frac{2K'\lambda^2}{E\gamma(1-m)} \end{aligned}$$

and  $E$  and  $\nu$  are the elastic modulus and Poisson's ratio of the shell material. The solution of Eqs. (1) is given by

$$\begin{aligned} \phi(\xi) &= M_1 \cosh e\xi \cos b\xi + M_2 \sinh e\xi \sin b\xi - \frac{\nu\gamma^2}{12(1-\nu^2)} \left(\frac{p}{E}\right) \left(1 - \frac{\gamma}{2\lambda}\right) \\ \tilde{\phi}(\tilde{\xi}) &= \tilde{M}_1 \cosh \tilde{e}\tilde{\xi} \cos \tilde{b}\tilde{\xi} + \tilde{M}_2 \sinh \tilde{e}\tilde{\xi} \sin \tilde{b}\tilde{\xi} + \tilde{M}_3 \cosh \tilde{e}\tilde{\xi} \sin \tilde{b}\tilde{\xi} + \tilde{M}_4 \sinh \tilde{e}\tilde{\xi} \cos \tilde{b}\tilde{\xi} \end{aligned} \quad (2)$$

in which

$$\begin{aligned} e, \tilde{e} &= (2)^{1/2}\eta \cos(\alpha/2), (2)^{1/2}\tilde{\eta} \cos(\tilde{\alpha}/2) \\ b, \tilde{b} &= (2)^{1/2}\eta \sin(\alpha/2), (2)^{1/2}\tilde{\eta} \sin(\tilde{\alpha}/2) \\ \alpha, \tilde{\alpha} &= \cos^{-1}\left(\frac{\eta^2}{\mu^2}\rho^2\right), \cos^{-1}\left(\frac{\tilde{\eta}^2}{\mu^2}\tilde{\rho}^2\right) \end{aligned}$$

The six constants of integration  $M_1, M_2, \tilde{M}_1, \dots, \tilde{M}_4$  are readily found by satisfying four continuity conditions at  $\xi = m$  and two boundary conditions at  $\tilde{\xi} = 1-m$ . The classical theory (Love's First Approximation) solution follows from Eqs. (2) by examining the limit  $\mu \rightarrow \infty$ .

### Results and Discussion

The abovementioned solution will now be illustrated by way of an example. Since we are primarily interested in flexure and the effects of support parameters on the stress resultants, we consider the problem shown in Fig. 1 with  $p = 10^{-5} E$ . The numerical computations were carried out on the computer and the results are shown in Figs. 2-5.

The effect of support width on axial moment distribution for a given value of support modulus ( $10^3$  psi) is shown in Fig. 2 where the predictions of both shear deformation theory and classical theory are plotted for  $(L/a) = 1.0$  and  $(h/a) = 0.3$ . As would be

Received December 26, 1973; revision received May 2, 1974.

Index categories: Structural Static Analysis; Structural Design, Optimal.

\* Physical Properties Research Department, Research and Development Laboratories; also Adjunct Associate Professor, Department of Theoretical and Applied Mechanics, Cornell University, Ithaca, N.Y.

† Naval Officer, Turkish Naval Academy.